inter.noise
27-30 AUGUST HONG KONG 2017

Generating a Position-Adaptive Quiet Zone in Enclosed Spaces

Sven HÖBER[1]; Christian PAPE[2]; Eduard REITHMEIER[3]

[1 2 3] Institute of Measurement and Automatic Control, Germany

ABSTRACT

When exposed to noise regularly and continuously, it becomes a severe threat for the human health. Hence, the control of noise is a contemporary and widely known issue, especially in contexts of work safety in the industrial environment, but as well in the domestic field. The most common solutions are based on passive control approaches, which either involve high monetary effort (when coupled with construction actions for example) or at least require persons to wear ear protection at all time. In recent years, however, there has been a remarkable increase in the development and application of active noise control solutions. Still, the problem remains that those solutions are often tailored to a certain setting or require costly modifications of the environment.

To overcome these limitations, this paper presents the concept of a position-adaptive noise control system, which aims to provide the attenuation of noise at a movable local quiet zone, that tracking the user's ears when moving within the workspace. This enables the control of noise at a spatially shifting location without any mobile devices to be carried. The application in offices or industrial settings for example – meaning in enclosed spaces – however incorporates the challenge of controlling sound in a large spatial range, influenced by reverberation. The associated need for an accurate transfer path modeling leads to the adjacent model prediction technique, presented in this paper.

Keywords: Active Noise Control, Adaptive Quiet Zone, Reverberant Room

1. INTRODUCTION

In recent years, a whole range of ANC products has become available for the consumer market, e.g. ANC headphones. But also the business or industrial section is offered a variety of ANC solutions for ducts, refrigerators or passenger cabins for example (1). However, these techniques either aim to reduce the noise emission globally, which is not always possible, or are tailored to a specified application. Moreover, in case of local noise reduction – referred to as quiet zone strategy (1) – one is spatially bound to the physical sensors that measure the resulting sound field.

The aim of this work is to generate a moving local quiet zone at an arbitrary spatial position without relocating the respective microphones. Moreau et al (2) dealt with this virtual sensing problem and presented various methods to attenuate noise aside the physical sensors. One method is the remote microphone technique (RMT), which predicts the sound pressure level at the virtual microphone using the secondary path models of the actual and the virtual error microphone as well as the transfer path of the primary disturbance between them. Regarding signal prediction, also a Kalman filter approach has been presented. Experimental results using the RMT and the Kalman filter for virtual sensing can be found in (3), (4) for example. However, unlike fixed setups, a moving position introduces continuously changing transfer paths that have to be tracked. Concerning this problem, also moving virtual sensing algorithms have been presented and experimentally investigated (2). Indeed, significant attenuation was achieved using these techniques, but only in a small range. The spatial range that the sensors, actuators and the final quiet zone are arranged in, shall be enlarged in this work. Since in a reverberant room sound propagates in a deterministic way in the lower frequency region (that is of interest for active control), it is practically predictable if the properties – the room acoustics – are well known. The active control of noise inside a room has previously been investigated in (5),

[1] sven.hoeber@imr.uni-hannover.de
[2] christian.pape@ imr.uni-hannover.de
[3] sekretariat@ imr.uni-hannover.de

already using FIR filtering. Further results, using the conventional FxLMS filtering with both feedforward and feedback control are presented in (6), (7) for example. Whereas Tseng et al (6) point out the limited possibilities of feedback control due to the high delays in rooms, Morgan and Thi (7) deal with the aspect of managing the high filter orders that emerge in room applications by the introduction of a subband ANC structure, later picked up again by Milani (8). Also, a summarizing investigation regarding enclosed space ANC can be found in (1).

All these results have been taken into consideration for the design of the proposed ANC system concept. The focus of this paper lies on the modeling part, the ANC structure itself will only be presented in theory. However, first of all, the properties of the environment, in which the sound field shall be controlled, are identified by analyzing the room acoustics in section 2.1. Then, in section 2.2, a simple ANC test setup is experimentally evaluated to initially show what attenuation can be achieved without special effort regarding the environment. Section 3 then presents the methods and setups proposed to handle the special challenges that emerge because of the room's acoustic influence and the wide spatial range the ANC system is aimed to operate within. The resulting adjacent model prediction technique is finally investigated in simulations in section 4.

2. PRELIMINARY INVESTIGATIONS

2.1 Room Acoustics

For the control of a sound field inside an enclosure, it is necessary to analyze its influence on the propagation of the sound. These properties are described by the room acoustics, which include the room geometry and the surface's reflection attributes for example (9), (10). To analyze the properties, it is usual to measure the room impulse response, which yields a parametric transfer function in the frequency domain that can be displayed in a Bode diagram. This way, it is possible to assess the number and shaping of the dominant modes that characterize the reverberant enclosure (10). Eventually, for the application of active noise control, these modes must be considered in the modeling of the respective transfer paths.

The test room used in this work consists of a rectangular, lightly damped cabin with a dimension of 2.8 x 2.8 x 2.4 m³. For the estimation of the test room impulse response $h(t)$, a loudspeaker – the excitation source – is placed near to the wall facing towards a microphone placed in the middle of the room. The impulse response is derived by means of the 2-channel FFT technique, which first involves the measurement of the frequency response $H(\omega)$ by exciting the room with a sweep signal. Then the test room impulse response is calculated by inverse Fourier transform according to

$$h(t) = \mathrm{IFFT}\{H(\omega)\} = \int_{-\infty}^{\infty} H(\omega)\, e^{j\omega t}\, d\omega\,. \tag{1}$$

To obtain impulse responses at different positions in the room, the microphone is successively moved away from the loudspeaker with a distance from 0.8 to 1.7 m. The results obtained at the starting position (0.8 m) and the end position (1.7 m) are depicted in Figure 1.

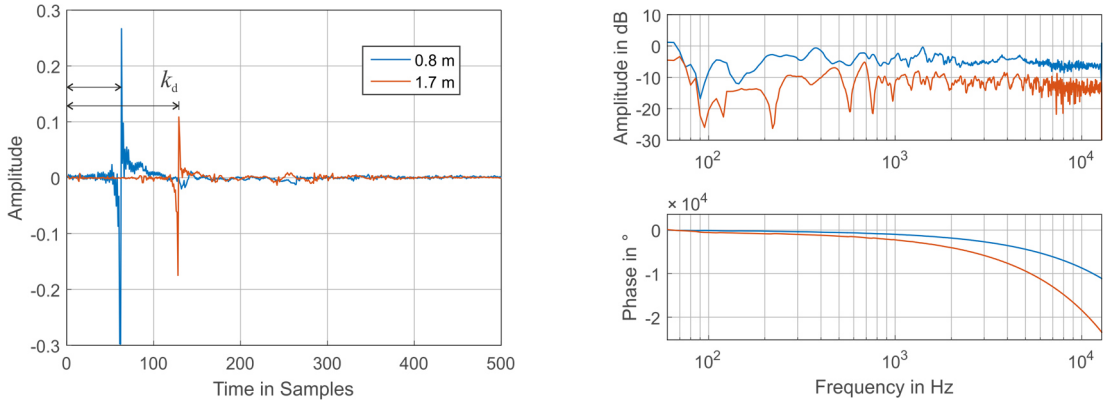

Figure 1 – Room impulse responses and Bode diagrams at the minimum and maximum distance

The first information to obtain from the impulse responses is the divergent delay k_d, which reflects the different distances to the source. Second, the maximum peak amplitude, determined by the direct sound impact, decreases with the distance as does the sound pressure level (additionally, in an

enclosure this is influenced by the reverberations as will be shown later). This information is also visible in the frequency response (on the right). Furthermore, it reveals the influence of the reverberant walls of the test room which become apparent in the lower frequency area below 1 kHz. Hence, a spatial shift has sensible effect on the propagation path that can be measured between the source and the sensor, thus making it challenging to set up an ANC system inside the room.

However, the frequency response will shape in respect to the room geometry (assumed to be constant) which makes it potentially predictable if the spatial position is known. To illustrate this, Figure 2 compares the room impulse responses measured at different distances with the initial delay omitted. The left plot shows that the first 40 samples are actually similar in shape, but the following area of samples is different for each distance. When displayed in three dimensions (on the right), it reveals that the latter area (in dotted lines) forms a notch-like pattern over distance. As can be seen, the notch moves in respect to the distance, but in no linear relation to it. This area reflects the influence of late reverberations (9) which thus depends on the distance to the walls.

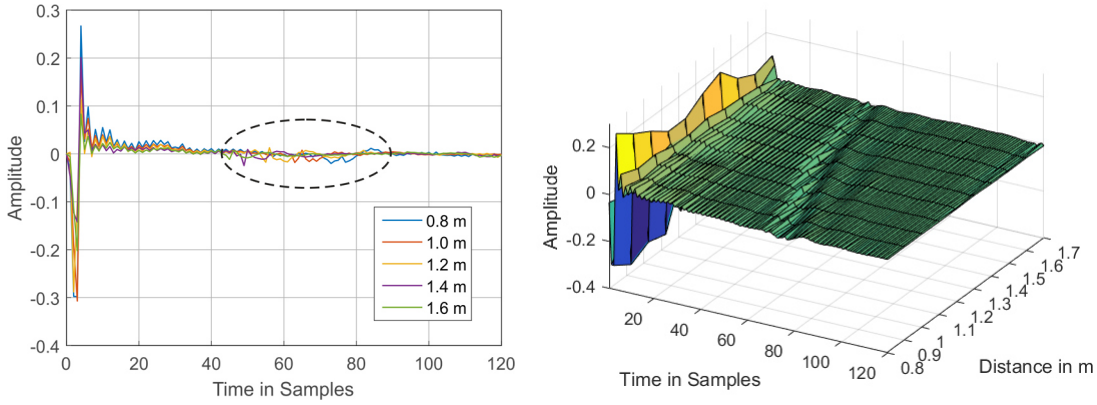

Figure 2 – Room impulse responses for different distances

Furthermore, it becomes apparent that the peak amplitudes also vary with different positions. This was already mentioned above when discussing the influence of the direct sound. Hence, the shape as well as the amplitude of the room impulse response are deterministic and can thus be estimated given that the spatial position is known and a priori information about the room acoustics (e.g. measurements) is available. These results and considerations will be picked up again in section 3.1. But first, the following section discusses a simple ANC setup for the creation of a spatially fixed quiet zone in the test room.

2.2 Control of Narrowband Sound

The preceding section has shown the influences of the room acoustics on the sound field and the air bound transfer paths, respectively. However, before taking this into account, a first setup for ANC in the test room is implemented to investigate the attenuation achievable without this information. It involves a simple SISO structure to reduce the sound pressure of narrowband noise (primary source) at a spatially fixed error microphone using a single loudspeaker (secondary source). This setup is shown in Figure 3. The equivalent block diagram of the system is depicted on the right.

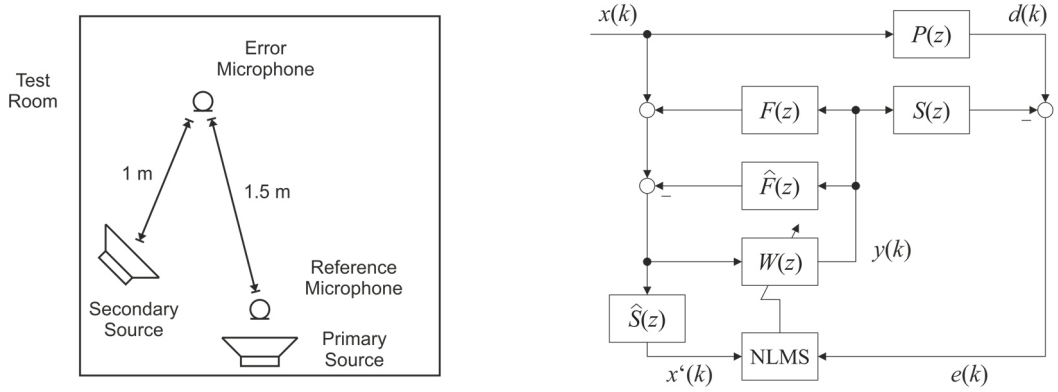

Figure 3 – Left: setup for ANC test. Right: block diagram of the implemented system

Basically, it consists of a feedforward control structure, that uses the normalized FxLMS algorithm to adapt the filter $W(z)$ according to the present disturbance $d(k)$. The resulting signal $y(k)$ drives the secondary source, which emits the anti-noise, while the reference signal $x(k)$ and the error signal $e(k)$ are measured by the correspondent microphones. The actually processed reference signal is previously reduced by any influence of the feedback path $F(z)$ using a model $\hat{F}(z)$ for compensation. Since the error microphone is spatially fixed in this setup, the model of the secondary path $\hat{S}(z)$ for the FxLMS algorithm can be estimated offline. For both the secondary and the feedback path models, a filter length of 120 taps is used, the adaptive filter $W(z)$ has a length of 10 taps.

The system is excited with a harmonic disturbance of 500 Hz, emitted by the primary source. The results obtained with the described ANC system are shown in Figure 4. It can be seen, that the sound pressure level (SPL) at the error microphone was successfully reduced by about 25 dB. However, besides the expected compensation of the fundamental frequency, the spectrum of the error signal reveals that the first three harmonics have been amplified instead. This is what derogates the achievable attenuation and leads to the overall result of only 25 dB attenuation.

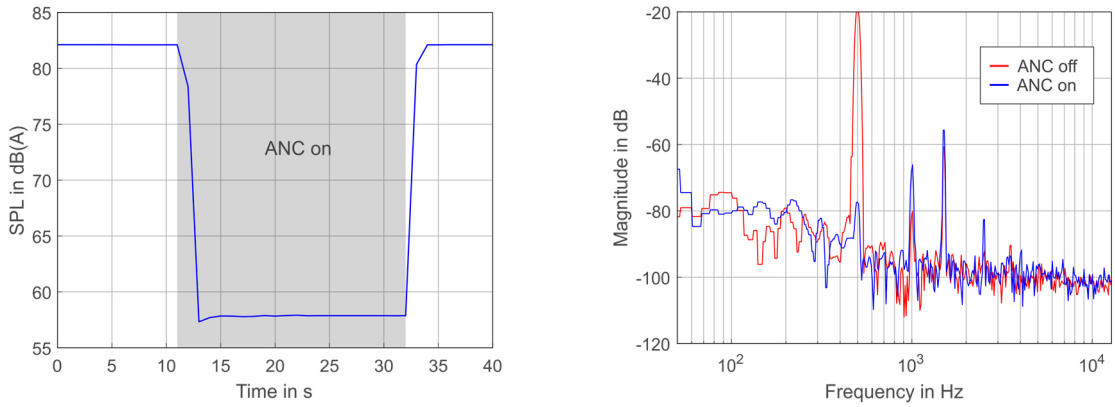

Figure 4 – Left: measured SPL at the error microphone. Right: measured error signal spectrum

On the one hand, the preceding results demonstrate that ANC in reverberant rooms is in principle possible with a minimum number of actuators and sensors and a conventional FxLMS adaptive filter implementation. However, the achievable noise reduction is limited because of increasing harmonics in the error spectrum. In addition, the quiet zone that has been created this way only exists for one position since the secondary path changes with every spatial shift. These issues are dealt with in the proposed ANC system design, which is topic of the next sections.

3. PROPOSED CONCEPT

3.1 Adjacent Model Prediction

Since the secondary path changes with every shift in position, it is necessary to first detect this change and second, update the model respectively. For this, the secondary path is modelled separately by its minimum-phase and all-pass part according to

$$\hat{S}(z) = \hat{S}_{\mathrm{mp}}(z) \cdot \hat{S}_{\mathrm{ap}}(z) = \hat{S}_{\mathrm{mp}}(z) \cdot z^{-k_{\mathrm{d}}} . \tag{2}$$

This decomposition reduces the length of the model FIR filter significantly, because the magnitude and phase distortion introduced by the secondary path are completely represented by the minimum-phase part $\hat{S}_{\mathrm{mp}}(z)$. The all-pass part contains the remaining pure propagation delay of the secondary path and is approximated simply using a discrete delay z^{-k_d}, which leads to the identification setup shown in Figure 5.

Hence, for the identification of the minimum-phase part, the delay must be known first. It is primarily dependent on the air propagation time the anti-noise sound waves need to travel from the secondary source (their origin) to the error microphone. Additionally, the delay is extended by the electrical components of the control system, mainly the in- and output modules containing the AD/DA converters. Since the hardware properties are expected to be constant whilst operating, the latter part of the delay can be estimated a priori. The first part, however, has to be estimated online every time the position of the quiet zone should change, which leads back to the beginning of this section – meaning the detection of a position change.

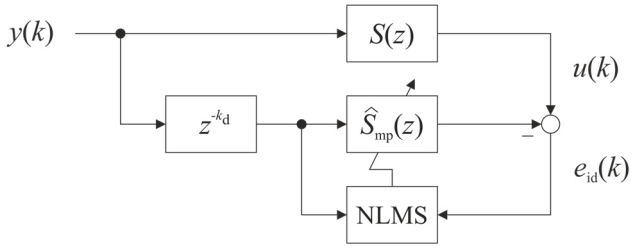

Figure 5 – Block diagram of the minimum-phase part identification

Since the error microphones shall be spatially fixed and thus not affected by the moving person, any approach incorporating the error microphone signal would fail. Hence, instead of using the acoustical sensors, an optical sensor approach is proposed. This means, a camera is used to track the person's head and ears, respectively, to first detect any movement – meaning a change of the secondary path – and directly determine the new position inside a preliminarily defined work space (Figure 6).

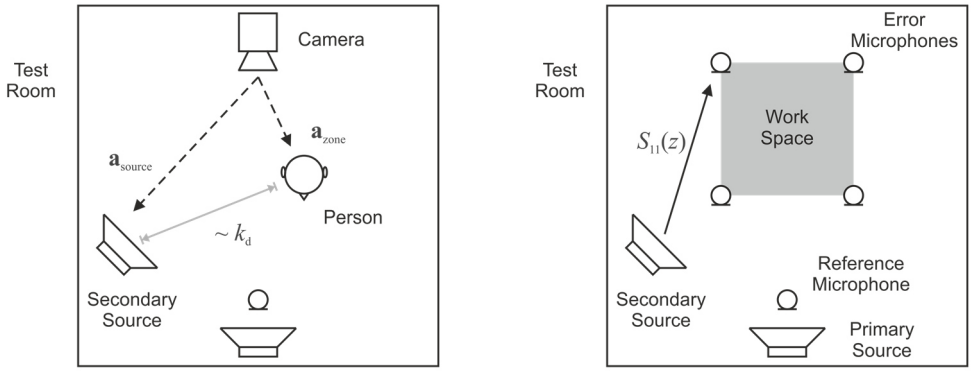

Figure 6 – Left: optical delay estimation. Right: setup for moving quiet zone ANC.

This way, knowing the position of the secondary source(s), it would be possible to derive the propagation time corresponding to the current position, where the quiet zone is finally aimed to be generated at. Given a nearly constant temperature inside the room the delay time can then be calculated according to

$$\hat{T}_{\mathrm{d,air}} = \frac{\left\| \mathbf{a}_{\mathrm{zone}} - \mathbf{a}_{\mathrm{source}} \right\|}{c_{\mathrm{air}}} \tag{3}$$

with $\mathbf{a}_{\mathrm{zone}}$ and $\mathbf{a}_{\mathrm{source}}$ being the 3-dimensional data vectors captured by the camera and c_{air} being the sound speed in air. At last, the delay in samples is obtained considering the sampling frequency with

$$k_{\mathrm{d}} = \hat{T}_{\mathrm{d,air}} \cdot f_{\mathrm{S}} \,. \tag{4}$$

Now, that the delay of the secondary path is continuously estimated, the minimum-phase part can be identified using the structure previously depicted in Figure 5 (for reasons of clarity, the minimum-phase part is simply referred to as secondary path in the following). Still, the problem remains that the error microphones provide no information about the sound field inside the defined work space, where no signal can actually be measured. Hence, that information has to be predicted using the available secondary path models at the fixed microphone positions

$$\mathbf{S}_{\mathrm{m}} = \begin{pmatrix} S_{11}(z) & S_{12}(z) \\ S_{21}(z) & S_{22}(z) \end{pmatrix}. \tag{5}$$

Furthermore, the results of the preliminary investigations can be used. In section 2.1, the room acoustics were analyzed by calculating the impulse responses at different equidistant positions, which correspond to the secondary paths $S_{xyz}(z)$ of the secondary source and the respective position (x,y,z). As pointed out, the transfer behavior of the air bound sound is determined by a certain pattern dependent on the acoustical properties of the room, that shall be used to predict the impulse response of positions aside the microphones, such that

$$S_{xyz}(z) = f(\mathbf{S}_{\mathrm{m}}, \mathbf{a}_{\mathrm{zone}}) \,. \tag{6}$$

Eventually, the system shall determine the current secondary path model automatically, according to the position data it obtains from the camera that tracks the person inside the work space. A simulation based investigation of this modeling approach with manually chosen positions within a one-dimensional range is presented in section 4. First, the following section deals with the actual ANC controller design.

3.2 ANC Structure

In the preceding chapter, it was shown that the problem of unknown transfer paths aside the error microphones can be overcome by the adjacent model prediction method. However, for an adaptive ANC system, the signal of the error microphone is still needed as a feedback for the adaption algorithm. If the secondary path model in the FxLMS structure does not correspond to the actual path at the microphone position, the algorithm will not converge. Hence, it is necessary to predict the error signal at the desired position. For this, the remote microphone technique is applied. The block diagram of the resulting ANC system structure is depicted in Figure 7.

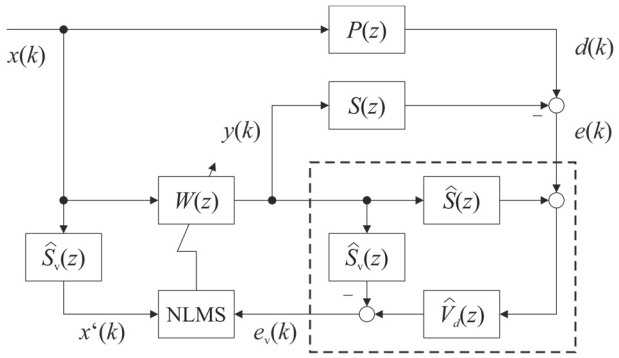

Figure 7 – Block diagram of the ANC system using remote microphone technique

Basically, it is the same ANC system as used in section 2.2. The feedback compensation is not shown. But instead of the actual error microphone, the target area for the quiet zone is now the virtual microphone, placed arbitrarily inside the work space. Hence, the LMS algorithm does not aim to minimize the actual error signal $e(k)$ (measured by the physical microphone), but the signal $e_{\mathrm{v}}(k)$ corresponding to the virtual microphone. It is estimated using the respective transfer paths that involve the physical and virtual microphone, e.g. the secondary paths $S(z)$ and $S_{\mathrm{v}}(z)$. The virtual disturbance path $V_d(z)$ connects the microphones according to

$$V_d(z) = \frac{D_{\mathrm{v}}(z)}{D(z)} = \frac{X(z)P_{\mathrm{v}}(z)}{X(z)P(z)} = \frac{P_{\mathrm{v}}(z)}{P(z)} \,. \tag{7}$$

with $P(z)$ and $P_{\mathrm{v}}(z)$ being the respective primary paths to the microphones. Hence, the transfer path models in the dotted box must be updated with every position shift. The secondary paths can be identified offline and estimated using the model prediction presented in section 3.1, respectively. The primary paths can in principle also be identified if there is the possibility to generate a proper excitation signal. However, this way the transfer function $V_d(z)$ becomes an IIR filter, which introduces potential stability problems. The better way is to estimate the virtual disturbance path directly as an adaptive filter $\hat{V}_d(z)$. For this, the disturbance is measured using the fixed error microphones before the ANC system is in operation. This is depicted in Figure 8.

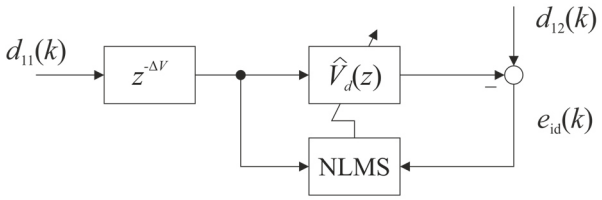

Figure 8 – Initial virtual disturbance path identification at microphone positions 11 and 12.

To only model the minimum-phase part, a discrete delay is inserted, which represents the run-time difference ΔV of the respective primary paths $P(z)$ and $P_v(z)$ to the microphones. After the initial identification, the virtual disturbance path model for an arbitrary virtual location can be predicted like the secondary path models.

The modeling technique for the estimation of the transfer path models that correspond to the virtual microphone positions was introduced in section 3.1. The next section will discuss this technique by means of simulation results. For investigations concerning the remote microphone technique, refer to (2).

4. SIMULATION RESULTS

The modeling approach presented in section 3.1 has been tested in simulations. This section shows the results and discusses what to consider for the actual implementation. It is based on calculating the analytical relation between the known secondary path models (corresponding to the spatially fixed error microphones) and the unknown transfer function of the virtual microphone moving within the work space. Eventually, the virtual secondary path model shall be predictable merely from the position data captured by the camera. This has been investigated in simulations using real identified models for the case of two physical microphones placed in line with the secondary source and 0.5 m apart; a third microphone is placed in between. This is depicted in Figure 9. Within this small distance, it is assumed that Equation 6 denotes a linear combination of the known models according to

$$s_c(k) = f(\mathbf{s}_{ab}) = \mathbf{s}_{ab}^{\mathrm{T}} \cdot \boldsymbol{\gamma} \tag{8}$$

with

$$\mathbf{s}_{ab} = \left[s_a(k) \;\; s_b(k)\right]^{\mathrm{T}}, \quad \boldsymbol{\gamma} = \left[\gamma_1 \;\; \gamma_2\right]^{\mathrm{T}}. \tag{9}$$

being the secondary path models corresponding to the error microphones and the parameter vector, respectively.

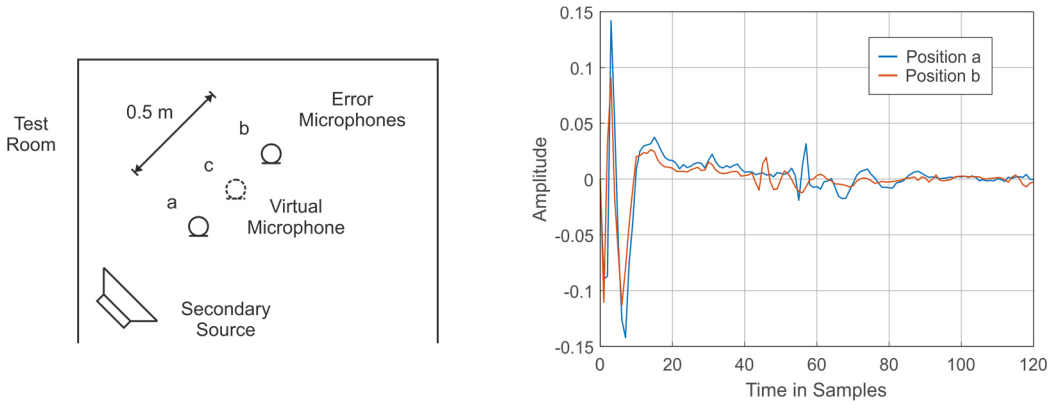

Figure 9 – Left: setup for model prediction. Right: identified impulse responses at positions a and b.

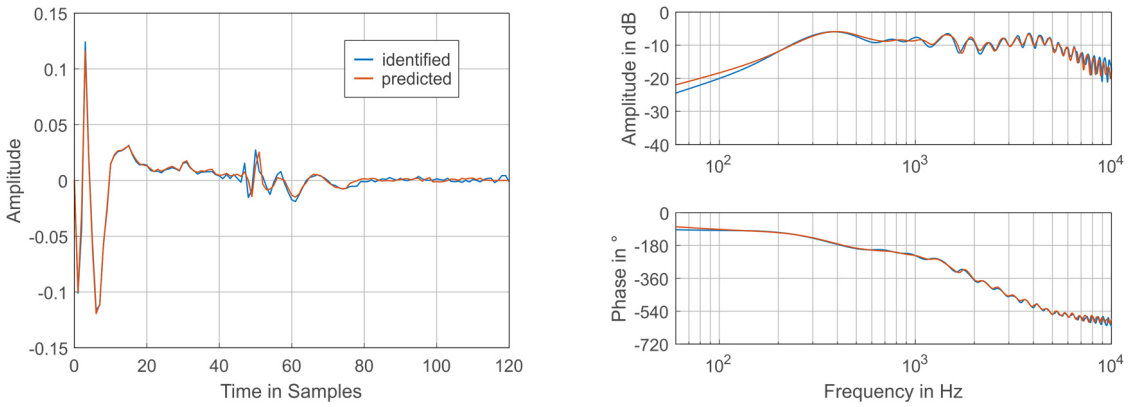

Figure 10 – Impulse response and Bode diagram of the secondary path model at position c ($\gamma_1 = 0.5$)

When setting $\gamma_2 = 1 - \gamma_1$, the predicted model $s_c(k)$ becomes a linear interpolation of the identified models $\mathbf{s}_{ab}$. However, as can be seen in Figure 9, the impulse responses corresponding to the physical microphones are only similar in shape for the first 40 samples (also see Figure 2). As already shown in section 2.1, this is because of the characteristic pattern representing late reverberations. Since the microphones are placed in different distances to the walls, their impulse responses differ in this area. Hence, before a linear interpolation is applied to this area, it is additionally necessary, to shift the weights according to

$$s_c(k) = [s_a(k) \;\; s_b(k+\Delta)] \cdot \boldsymbol{\gamma} \quad \forall k > 40\,, \tag{10}$$

with Δ reflecting the difference in samples between the respective areas of the two impulse responses. This algorithm is now tested by applying it to the setup depicted in Figure 9. Position c is set in the center between the positions a and b, thus the distance is 0.25 m. The corresponding secondary path $S_c(z)$ is initially identified as usual. Then the physical microphone is removed. Figure 9 shows the identified impulse responses of the secondary paths from the source to the microphones at the positions a and b. To predict the secondary path corresponding to the microphone virtually placed at the center position c, we set $\gamma_1 = 0.5$. The result is displayed in Figure 10. As can be seen, the impulse response of the virtual microphone, that has been derived using the proposed interpolation, is similar to the impulse response identified before with the physical microphone at that position. This is also reflected by the frequency response of the respective models. The Bode diagram reveals almost no differences in magnitude and phase between the identified and the virtual model. To further validate the method of the model interpolation, the virtual microphone is now moved to other positions between the fixes microphones. With position c marking the half-path length, the microphone is now also placed at the quarter (position d) and the three-quarter path length (position e). Accordingly the parameter γ is set to 0.25 and 0.75, respectively. The results of the model prediction at these two positions are shown in Figure 11. Again, the prediction fits the identification except for slight differences in amplitude; the basic shape of the impulse response is modelled accurately.

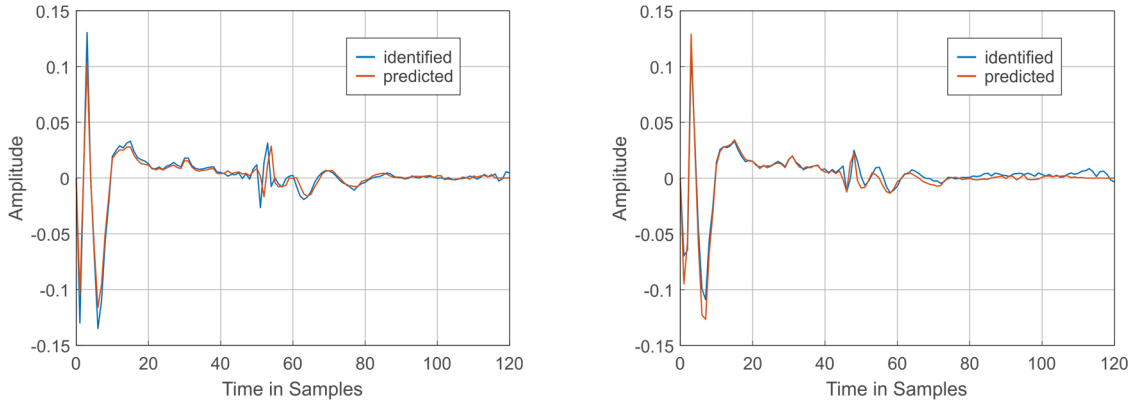

Figure 11 – Impulse response of the secondary path model at positions d (left) and e (right)

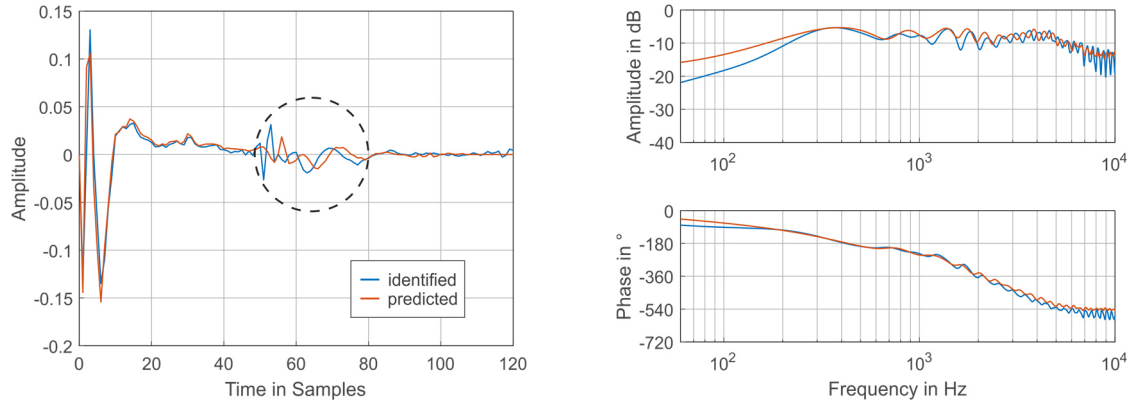

Figure 12 – Secondary path model at position c with extended distance between microphones

To test the limits for the linear interpolation, the distance between the physical microphones is now extended to 1 m. Again, using the secondary path models corresponding to the previously shifted

positions a and b, the model at position c is to be predicted using the linear interpolation according to Equations 9, 10 (setting $\gamma = 0.5$). Figure 12 shows the obtained impulse response as well as the frequency response of the models with this setup. When compared to the previous setup (see Figure 9), differences between the identified and the predicted model become apparent. While the first half of the impulse response is still accurate, the pattern in the middle is predicted with a displacement. The Bode diagram reveals, that this modeling error mainly effects the higher frequency range, but also causes deviations especially in amplitude below 300 Hz. These results show that the linear interpolation is only feasible within a limited spatial range. For an enlargement of the spatial range, meaning the work space respectively, the usage of higher order or trigonometric functions is necessary. This aspect is picked up again in the following conclusion.

5. CONCLUSIONS

This paper dealt with the design of a position-adaptive ANC system to generate a moving quiet zone inside a reverberant room by tracking the person moving within a respective work space. It shall adapt to variations of the transfer paths by means of an optical delay estimation combined with a model prediction method based on the characteristic sound field formation.

To first assess the properties of the test room, its room acoustics have been analyzed using impulse responses derived from measured frequency domain data. It has shown, that the room acoustics introduce a characteristic pattern into the impulse responses, which could be used for the prediction of transfer paths at an arbitrary position. This lead to the proposed adjacent model prediction technique, which incorporates the interpolation of the filter weights of adjacent transfer path models according to the characteristic sound field. The position of the desired quiet zone is initially tracked by a camera, that eventually yields the according delay used to determine the respective secondary path. Eventually, the quiet zone shall be generated by using the remote microphone technique. The simulation results have shown, that with the proposed modeling method it is possible to estimate the secondary path transfer function at a basically arbitrary position without directly measuring the local sound field. This necessary information is derived from spatially fixed microphones, whose secondary paths are identified online and thus can track variations in the setting.

In future work, the analytical combination of the physically identified transfer paths shall be calculated using neural networks that are trained in respect to the sound field and the resulting impulse response pattern in a preliminary stage. This way, the work space could be enlarged. Furthermore, the ANC part shall be implemented using a subband structure (see (6), (8)) to reduce the filter order and enable the attenuation of broadband noise. For the compensation of the harmonics, discussed in section 2.2, an additional, static feedback controller is contemplated.

REFERENCES

1. Kuo SM, Morgan DR. Active Noise Control Systems: Algorithms and DSP Implementations. New York, NY, USA: John Wiley & Sons, Inc.; 1996.
2. Moreau D, Cazzolato BS, Zander AC, Petersen CD. A review of virtual sensing algorithms for active noise control. Algorithms. 2008; (1): 69-99.
3. Booij PS, Berkhoff AP. Virtual sensors for local, three dimensional, broadband multiple-channel active noise control and the effects on the quiet zones. Proc ISMA 2010; 20-22 September 2010; Leuven, Belgium 2010. p. 151-65.
4. Petersen CD, Fraanje R, Cazzolato BS, Zander AC, Hansen CH. A Kalman filter approach to virtual sensing for active noise control. Mechanical Systems and Signal Processing. 2008; (22): 490-508.
5. Miyoshi M, Kaneda Y. Inverse filtering of room acoustics. IEEE Transactions on Acoustics, Speech, and Signal Processing. 1988; 36(2): 145-52.
6. Morgan DR, Thi JC. A delayless subband adaptive filter architecture. IEEE Transactions on Signal Processing. 1995; 43(8): 1819-30.
7. Tseng WK, Rafaely B, Elliot SJ. Combined feedback-feedforward active control of sound in a room. J Acoust Soc Am. 1998; 104(6): 3417-25.
8. Milani AA, Panahi IMS, Loizou PC. A new delayless subband adaptive filtering algorithm for active noise control systems. IEEE Transactions on Audio, Speech, and Language Processing. 2009; 17(5): 1038-45.
9. Kuo SM, Lee BH, Tian W. Real-Time Digital Signal Processing. Chichester, West Sussex, UK: John Wiley & Sons, Ltd; 2013.
10. Snyder SD. Active Noise Control Primer. New York, NY, USA: Springer Science + Business Media; 2000.